R. REBHI[1]
P. MATHEY[1,✉]
M. GRAPINET[1]
H.-R. JAUSLIN[1]
S. ODOULOV[2]

Phase mismatch effects on the dynamics of a semilinear photorefractive oscillator with reflection-type gratings

[1] Institut Carnot de Bourgogne, UMR 5209 CNRS-Université de Bourgogne, 9 Avenue Alain Savary,
BP 47870, 21078 Dijon Cedex, France
[2] Institute of Physics, National Academy of Sciences, 46 Science Avenue, 03650 Kiev, Ukraine

ABSTRACT This paper describes the effect of pump waves misalignement on the performance of the semilinear photorefractive coherent oscillator with the reflection gratings. The oscillation intensity and its modulation frequency are calculated numerically for different misalignement angles, coupling strengths and pump intensity ratios. It is shown that a small angular detuning of the pump wave, less than one milliradian, extends the range of pump ratios and the range of coupling strengths for which a non-degenerate oscillation occurs. The results of experiments with the $BaTiO_3$-based semilinear oscillator are in qualitative agreement with the calculated data.

PACS 42.65.Hw; 42.70.Nq; 42.65.Sf

1   Introduction

Photorefractive materials display strong optical non-linearity over a wide range of wavelengths, which manifests itself even for the relatively weak intensities of the interacting beams. Among the applications of photorefractive crystals, based on two or four-wave mixing are the correction of aberrations, the coherent coupling of laser beams, the coherent light amplification and the implementation of phase conjugate mirrors. The interest in phase conjugation has been extended to photorefractive oscillators and led to a deeper understanding of their features, especially their transverse pattern control and their dynamics. The first photorefractive oscillator was demonstrated with a $BaTiO_3$ crystal, many other oscillators were later designed with different geometries and different photorefractive materials [1, 2]. Photorefractive crystals with high two-beam coupling gain factor are needed to ensure the build-up of a coherent oscillation. For this reason, materials with high electro-optic coefficients and high trap densities are of special interest [3]. It has been pointed out also that in some cases the efficiency of the four-wave mixing and the phase conjugate reflectivity can be enhanced by misaligning the pump waves [4, 5]. We are interested in this paper in the dynamics of the semilinear coherent oscillator in a reflection grating configuration. Previous theoretical studies with this oscillator claimed that within the plane wave

approximation a non-degenerate oscillation is possible for a coupling strength greater than 2π [6, 7], while this behavior is observed experimentally with a lower value of the coupling strength [8, 9]. In this work, we extend the theoretical framework and show that an inexact alignment of the two pump waves results in a decrease of the threshold value below the value of 2π. In such a way one possible reason is revealed for the discrepancy mentioned above.

This paper is organized as follows: in Sect. 2, we present the semilinear oscillator with perfectly counterpropagating pump waves, we recall the equations of the model and the condition to obtain a non-degenerate oscillation. In Sect. 3, the set of dynamic equations is generalized for the case of small misalignment of the two pump waves of the considered coherent oscillator. The numerical simulations that follow reveal the influence of the pump beam misalignment on the oscillation dynamics. Finally, in Sect. 4, the comparison with the experimental results confirms the most important conclusions of numerical calculations.

2   The semilinear oscillator

2.1   *Principle*

The schematic representation of the oscillator under consideration is shown in Fig. 1. It is based on four-wave mixing in a photorefractive crystal pumped with two counterpropagating waves. The photorefractive crystal with the length l serves as a phase conjugate mirror and forms together with the conventional mirror M a semilinear photorefractive oscillator.

The build-up of oscillation waves in the cavity can be qualitatively explained in the following way: the pump wave 2 is scattered from optical imperfections inside the crystal. A part of this scattered radiation is reflected by the conventional mirror M (see Fig. 1) back into the crystal and interferes with pump 1 to generate a first grating with a low contrast. This grating diffracts wave 2 into wave 3 that interferes with pump 2 and generates another grating with the same period and orientation as the previous one but spatially shifted. Wave 3 reflected by the mirror M contributes to create a grating with a higher contrast in the photorefractive crystal. Step by step, waves 3 and 4 gain intensity and the grating amplitude increases until the process saturates. The dynamics of the system depends on parameters like the pump intensity ratio $r = I_2/I_1$, the coupling strength γl and the reflectivity R

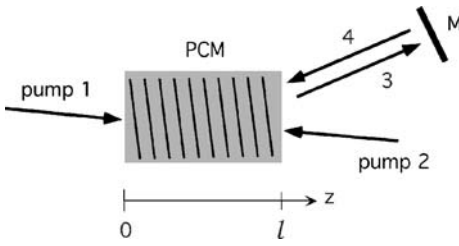✉ Fax: +33-380-395961, E-mail: pmathey@u-bourgogne.fr

FIGURE 1   Schematic representation of the semilinear oscillator with two counterpropagating pump waves. PCM is the photorefractive phase conjugate mirror, M is the conventional mirror. Fringes inside the sample show the structure of the reflection photorefractive grating

of the conventional mirror. To be within the single-grating approximation all interacting beams (1–4) must record only one grating in the crystal. This is achieved by appropriate choice of the beam paths to ensure the coherence between the pairs of beams (1,4) and (2,3) only. The four-wave mixing can also be interpreted in terms of real time holography where waves 1 and 4 write a hologram, wave 2 reads the hologram and is diffracted into wave 3. These two last waves record their own grating which is out of phase with respect to the grating written by waves 1 and 4. For this reason an imbalance between the pump wave intensities is needed for the oscillation build-up otherwise the seed beams will not initiate the process.

2.2   *Coupled wave equations*

Within a plane wave approximation and for slowly varying amplitudes, the system is described by a set of coupled wave equations (1)–(4) for the complex amplitudes of the interacting waves, and by (5), which describes the temporal variation of the grating amplitude [2, 6, 7]:

$$\frac{\partial A_1}{\partial z} = v^* A_4 \,, \tag{1}$$

$$\frac{\partial A_2}{\partial z} = v A_3 \,, \tag{2}$$

$$\frac{\partial A_3}{\partial z} = v^* A_2 \,, \tag{3}$$

$$\frac{\partial A_4}{\partial z} = v A_1 \,, \tag{4}$$

$$\tau \frac{\partial v}{\partial t} + v = \frac{\gamma^*}{I_0} \left(A_1^* A_4 + A_2 A_3^* \right) , \tag{5}$$

where z is the coordinate along the propagation axis, A_i are the complex amplitudes of the waves $i = 1, 2, 3, 4$; A_i^* are their complex conjugates, v is the magnitude of the grating, I_0 is the total intensity $I_0 = |A_1|^2 + |A_2|^2 + |A_3|^2 + |A_4|^2$, and τ is the response time of the photorefractive medium.

The boundary conditions for the considered semilinear oscillator are:

$$A_4(z = l, t) = \sqrt{R} A_3(z = l, t) \,, \tag{6}$$

$$A_3(z = 0, t) = 0 \,, \tag{7}$$

$$A_2(z = l, t) = \text{const.} \,, \tag{8}$$

$$A_1(z = 0, t) = \text{const.} \,, \tag{9}$$

where R is the reflectivity of the conventional mirror.

2.3   *Temporal intensity modulation in the cavity*

In this paragraph we recall the conditions for the existence of non-degenerate oscillations with perfectly aligned pump beams [6].

Considering the four wave mixing within the undepleted pump approximation, the pump waves are constant inside the crystal: $A_1(z) = A_1(z = 0)$ and $A_2(z) = A_2(z = l)$ so that the coupled wave equations (3)–(5) admit solutions of the form:

$$A_3(z, t) = A_3^+(z) \exp(+\mathrm{i}\Omega t) \,, \tag{10}$$

$$A_4(z, t) = A_4^-(z) \exp(-\mathrm{i}\Omega t) \,, \tag{11}$$

$$v(z, t) = v^-(z) \exp(-\mathrm{i}\Omega t) \,, \tag{12}$$

where Ω is a possible frequency detuning of the waves.

The phase conjugate reflectivity of the crystal is defined as:

$$\varrho(\Omega) = A_3^{+*}(l) / A_4^-(l) \,. \tag{13}$$

In the semilinear oscillator the oscillation waves manifest a frequency detuning for appropriately chosen values of the parameters like the coupling strength, the beam ratio or the conventional mirror reflectivity. Due to the feedback introduced by the conventional mirror any detuning Ω of wave 3 is present also in wave 4 since this last one is reflected by the classical mirror. Moreover, wave 3 being the phase conjugate of wave 4, a detuning $+\Omega$ of the first wave will result in the opposite detuning $-\Omega$ of the second wave: this is inherent to the principle of phase conjugation. If only one detuning ($+\Omega$ or $-\Omega$) is considered for each wave inside the cavity the boundary conditions (6)–(9) are not satisfied. Consequently, to retrieve the intensity modulation inside the cavity, the amplitudes of waves 3 and 4 are written as:

$$A_{3,4}(z, t) = A_{3,4}^+(z) \exp(+\mathrm{i}\Omega t) + A_{3,4}^-(z) \exp(-\mathrm{i}\Omega t) \,. \tag{14}$$

The amplitude of the grating v also contains the two components of the detuning:

$$v(z, t) = v^+(z) \exp(+\mathrm{i}\Omega t) + v^-(z) \exp(-\mathrm{i}\Omega t) \,. \tag{15}$$

Two conditions are required for the existence of the oscillation: first, the gain of the phase conjugate mirror must balance the feedback mirror reflectivity and second, the self reproducibility (in phase) of the waves (3,4) after a round trip in the cavity. Both conditions are expressed by the following equation:

$$\varrho(\Omega)\varrho^*(-\Omega) R = 1 \,. \tag{16}$$

Previous theoretical investigations showed that this equation admits non-degenerate solutions ($\Omega \neq 0$) if the coupling strength γl is greater than 2π [6].

However the temporal modulation of the intensity is observed experimentally with photorefractive crystals that do not ensure such a high coupling strength. The following section shows that the angular deviation from collinearity of the pump waves affects strongly the dynamics of the system: in the case of slightly tilted pump waves a non-degenerate oscillation may occur even for relatively low values of the coupling strength, smaller than 2π.

3 Misalignement of pump waves

3.1 Effect of misalignement on the recorded gratings

We study in this section the effects of a small misalignment of the pump waves on the dynamics of the oscillator. The considered situation is depicted in Fig. 2: The pump beams are not perfectly counterpropagating, the corresponding wave vector diagram for which there is no Bragg match $(\mathbf{k}_1 + \mathbf{k}_2 - \mathbf{k}_3 - \mathbf{k}_4 \neq \mathbf{0})$ is shown in Fig. 3. The Bragg diffraction process implies that waves 3 and 4 are also not collinear (see Fig. 3); waves (1,4) and (2,3) record two gratings with the same orientation but slightly different spatial frequencies. A fundamental difference, when compared to the case of collinear pump beams, is that the two gratings are no longer exactly out of phase and their mutual phase shift depends on the position within the photorefractive medium. This comes from the fact that the angle between waves 1, 4 is different from that between the waves 2, 3 so that the two gratings have different spacings.

A one-dimensional model is considered where all the spatial variations are along the z axis so that the relevant off-Bragg component is along the z axis. The relative spatial phase also called phase mismatch between the gratings is:

$$\Phi = \mathbf{\Delta}z = \Delta z \,, \tag{17}$$

where the off-Bragg parameter Δ is the modulus of $\mathbf{\Delta} = \mathbf{K}_{1,4} + \mathbf{K}_{2,3}$ with $\mathbf{K}_{1,4} = \mathbf{k}_1 - \mathbf{k}_4$ and $\mathbf{K}_{2,3} = \mathbf{k}_2 - \mathbf{k}_3$ the grating vectors.

3.2 Dynamic equations for nearly phase matched mixing

For the reflection grating geometry, the coupled wave equations at steady-state in the case of a phase mismatch are [4]:

$$\frac{\partial A_1}{\partial z} = \frac{\gamma}{I_0} \left[A_1 A_4^* + A_2^* A_3 \exp(\mathrm{i}\Delta z) \right] A_4 \,, \tag{18}$$

$$\frac{\partial A_2}{\partial z} = \frac{\gamma^*}{I_0} \left[A_1^* A_4 \exp(\mathrm{i}\Delta z) + A_2 A_3^* \right] A_3 \,, \tag{19}$$

$$\frac{\partial A_3}{\partial z} = \frac{\gamma}{I_0} \left[A_1 A_4^* \exp(-\mathrm{i}\Delta z) + A_2^* A_3 \right] A_2 \,, \tag{20}$$

$$\frac{\partial A_4}{\partial z} = \frac{\gamma^*}{I_0} \left[A_1^* A_4 + A_2 A_3^* \exp(-\mathrm{i}\Delta z) \right] A_1 \,. \tag{21}$$

We supplement these known equations with one that describes the temporal evolution of grating amplitude ν and
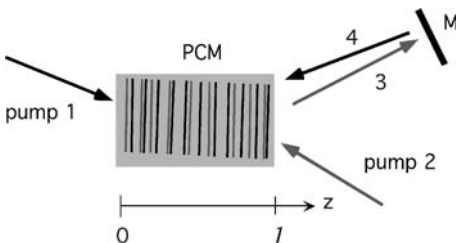

FIGURE 2 Schematic representation of pump misalignment. The two index gratings with the emphasized difference in grating spacings are shown
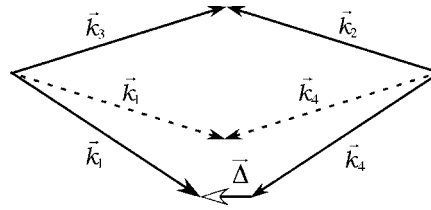

FIGURE 3 Wave vector diagram showing the deviation from collinear alignment. The *dashed wave vectors* represent the case of exact alignment where the Bragg condition is fulfilled

recreate them in the following way:

$$\frac{\partial A_1}{\partial z} = \nu^* \exp\left(\mathrm{i}\frac{\Delta z}{2}\right) A_4 \tag{22}$$

$$\frac{\partial A_2}{\partial z} = \nu \exp\left(\mathrm{i}\frac{\Delta z}{2}\right) A_3 \tag{23}$$

$$\frac{\partial A_3}{\partial z} = \nu^* \exp\left(-\mathrm{i}\frac{\Delta z}{2}\right) A_2 \tag{24}$$

$$\frac{\partial A_4}{\partial z} = \nu \exp\left(-\mathrm{i}\frac{\Delta z}{2}\right) A_1 \tag{25}$$

$$\tau \frac{\partial \nu}{\partial t} + \nu = \frac{\gamma^*}{I_0} \left[A_1^* A_4 \exp\left(\mathrm{i}\frac{\Delta z}{2}\right) + A_2 A_3^* \exp\left(-\mathrm{i}\frac{\Delta z}{2}\right) \right] \,. \tag{26}$$

The conservation laws

$$I_1(z, t) - I_4(z, t) = d_1 \,, \quad I_2(z, t) - I_3(z, t) = d_2 \tag{27}$$

are valid for (22)–(26).

Equations (22)–(26) are an extension of those given in [4, 10]; they take into account the pump beams depletion and the temporal evolution of the wave amplitudes and the index grating. They coincide with those considered in [11, 12] if Δ is set to zero.

3.3 Numerical solution

Equations (22)–(26) are solved numerically with the method described in [11]. Several simulations for different reasonable sets of parameters close to the experimental conditions have been performed and led to the following conclusion: In the presence of a small misalignment a non-degenerate oscillation occurs for coupling strengths γl smaller than the minimum threshold 2π estimated for the case of perfectly aligned pump waves [6]. An example of such behavior is illustrated in Fig. 4: the temporal variations of the oscillation intensity is plotted for a dimensionless detuning $\Delta l = 4.4$, a conventional mirror reflectivity $R = 0.05$, and a pump ratio $r = 2$.

For the same set of parameters but with perfectly aligned pump waves ($\Delta l = 0$) the simulation shows an identically zero intensity I_3 even for much longer exposure times, i.e., the oscillation does not occur.

The pump ratio being fixed, the coupling strength γl and the off-Bragg parameter Δ are two relevant variables that determine the dynamics of the system. To analyze the influence of the latter, we calculate the beat frequency and the
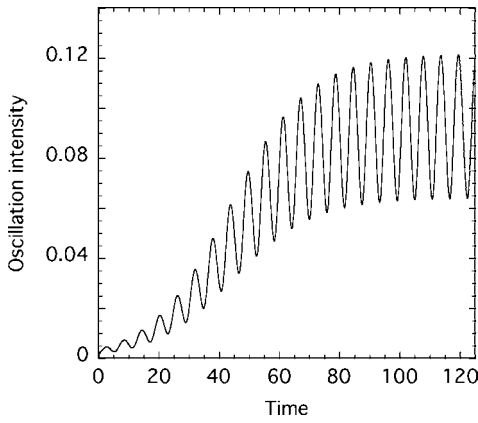
FIGURE 4 Numerically calculated intensity of wave 3 with the parameters $R = 0.05$, $r = 2$, $\gamma l = 4.35$, $\Delta l = 4.4$. The time is given in units of the response time of the material τ

intensity of the oscillation. Some representative examples are drawn with three dimensional plots in Figs. 5–7. The misalignment Δl is dimensionless in these graphs, l being the interaction length inside the sample. For a typical experimental geometry like that described in [12] (pump incidence angle about 30°, oscillation wave incidence angle about 45°, index of refraction about 2.4) the misalignment angle is $\Psi \simeq 0.25 \Delta l$ mrad.

The 3D plot in Fig. 5a displays the beat frequency 2Ω of the oscillation intensity as a function of Δl and the coupling strength γl for $R = 0.3$, $r = 2$, while Fig. 5b shows the corresponding intensity of the oscillation.

Figure 5a clearly shows that the range of the off-Bragg parameter for which the intensity modulation exists is larger for increasing γl. For the chosen values of the feedback mirror reflectivity and pump ratio, there exists a range for the off-Bragg parameter within which the oscillation intensity is modulated for coupling strengths $\gamma l \geq 4.5$. For $\gamma l \geq 2\pi$ we retrieve the known result that the oscillation intensity is temporally modulated even for perfectly counterpropagating pump beams ($\Delta = 0$). Figure 5a also shows that the beat frequency varies with Δl for any given coupling strength. Starting from a perfect phase matching ($\Delta l = 0$), the minimum mismatch necessary to obtain a non-degenerate oscillation increases as the coupling strength decreases. Figure 5b shows that pump misalignment can significantly enhance the oscillation intensity whatever the regime (degenerate or non-degenerate). This could be expected from the known enhancement of the phase conjugate reflectivity by angular deviation from collinearity of the pump waves [4, 5]. The transition from the degenerate to non-degenerate modes of oscillation appears clearly with the presence of a valley in the 3D plot.

For large pump misalignment the oscillation does not occur, at $\gamma l \leq 5.5$ it disappears for $\Delta l \leq 10$, which corresponds roughly to an angular detuning of $\Psi \leq 2.5$ mrad of the pump wave. At higher coupling strengths the isolated domains of frequency degenerate oscillation appear also for $\Delta l \geq 10$ (not shown in Fig. 5). The increase of the pump ratio leads to a smaller threshold for frequency degenerate oscillation. With $r = 4$ and $R = 0.3$, for example, the frequency degenerate oscillation occurs for $\gamma l \geq 4.2$ at $\Delta l = 0$ (Fig. 6). Its threshold
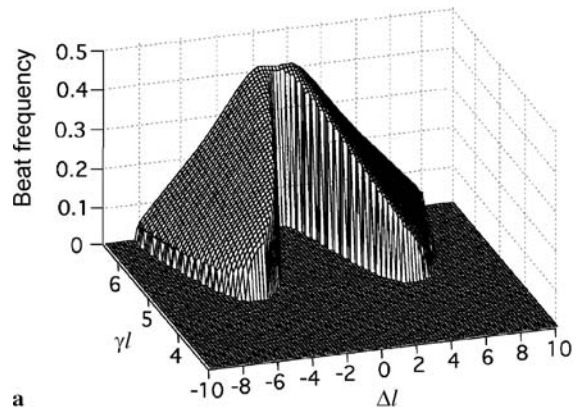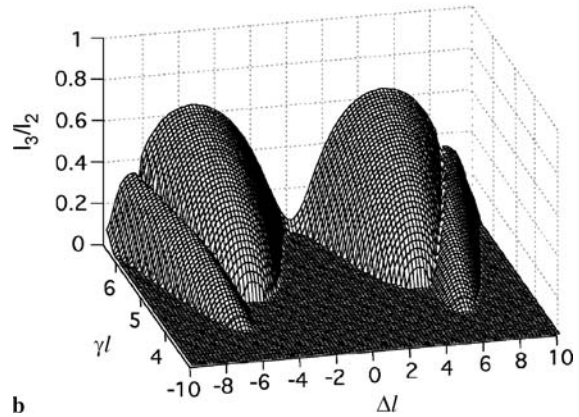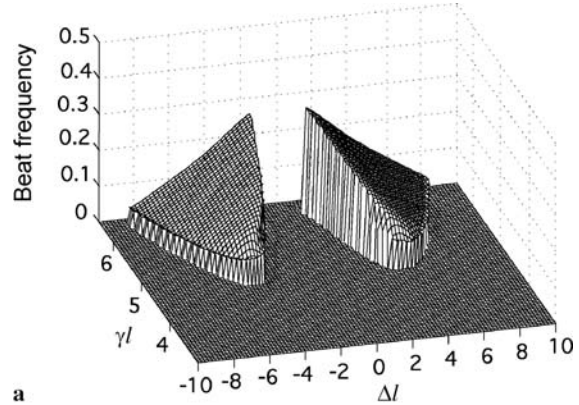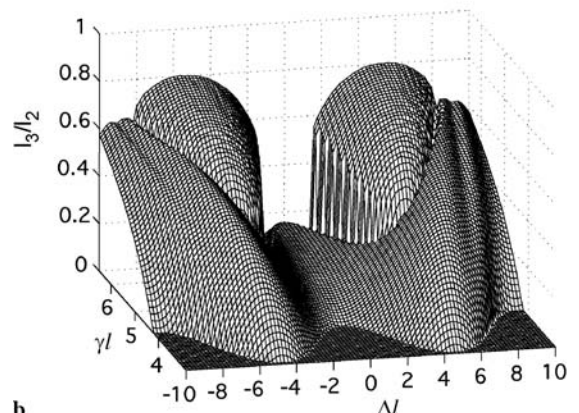

FIGURE 5 Beat frequency (**a**) and oscillation intensity (**b**) vs. the coupling strength γl and Δl for $R = 0.3$, $r = 2$

FIGURE 6 Beat frequency (**a**) and corresponding oscillation intensity (**b**) vs. the coupling strength γl and Δl for $R = 0.3$, $r = 4$
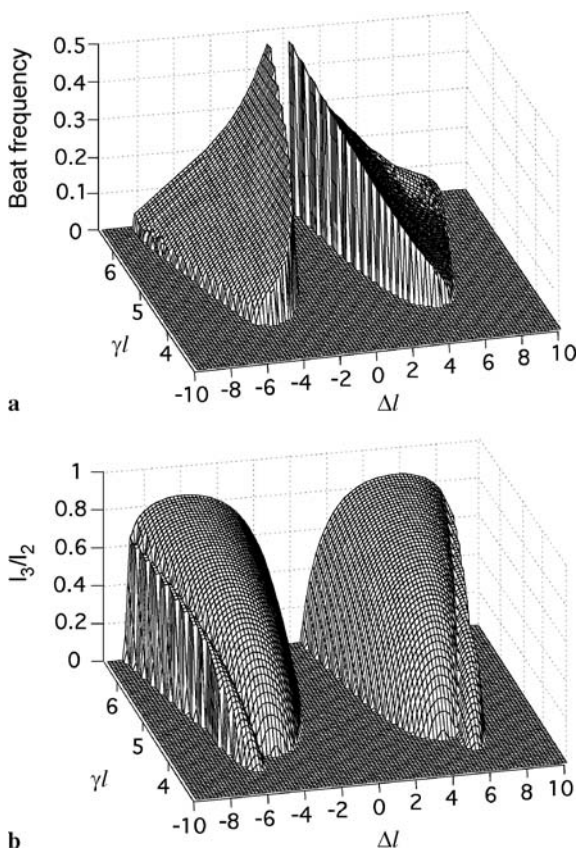
FIGURE 7   Beat frequency (**a**) and corresponding oscillation intensity (**b**) vs. the coupling strength γl and Δl for $R = 0.04$, $r = 4$

FIGURE 8   Calculated dependence of the oscillation spectrum on the pump ratio, with the parameters $R = 0.01$, $\gamma l = 4.35$, $\Delta l = 4.3$

FIGURE 9   Areas of existence of a non-degenerate oscillation for various coupling strengths and conventional mirror reflectivities in the case of perfect phase matching (*gray color*) and in the case of misalignment of $\Delta l = 5$ (*gray color* plus *light gray color*). The pump ratio is $r = 2$

drops down to $\gamma l = 3$ at $\Delta l = \pm 5$. Thus, for $\gamma l \simeq 4$ the oscillation is possible within the range of misalignment from $\Delta l = -8.6$ till $\Delta l = +8.6$ and it is frequency degenerate. Additional isolated domains of the degenerate oscillation appear at larger misalignment values for larger coupling strength. In comparison with Fig. 5, a higher coupling strength is necessary to obtain a bifurcation in the oscillation spectra. For strong imbalance of the pump intensities ($r \geq 500$) the bifurcation can hardly be observed unless one chooses a very high coupling strength.

To give an idea of the influence of the mirror reflectivity R, we present similar results in Fig. 7 obtained with a smaller mirror reflectivity of $R = 0.04$. The effects are clear: higher coupling strengths are required to obtain a non-degenerate oscillation for values of Δl that are close to the perfect alignment. Furthermore, the oscillation (both degenerate and non-degenerate) exists in a narrower range of Δl. The minimum coupling strength necessary to the onset of a non-degenerate oscillation becomes, on the contrary, smaller than that for $R = 0.3$, and it appears for a Δl value close to the preceding one.

From the dependencies obtained for different pump ratios r like those shown in Figs. 5–7 the bifurcation diagrams of the oscillation beat frequency are plotted (see, e.g., Fig. 8). For reference, note that with no misalignment the oscillation remains single-frequency throughout the whole range of r values where it exists.

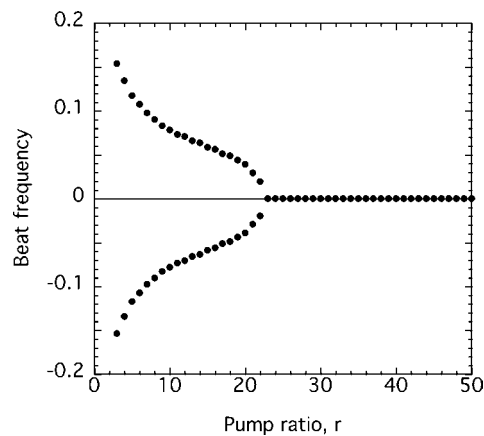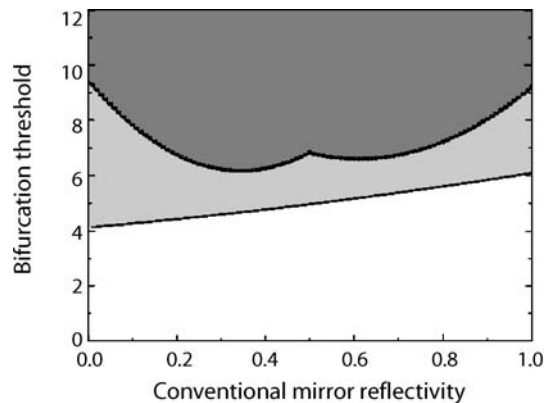Figure 9 summarizes the effect of the pump misalignment on the threshold of bifurcation in the oscillation spectrum. The threshold value of the coupling strength is shown as a function of the conventional mirror reflectivity for a pump intensity ratio of $r = 2$ and for two values of the dimensionless detuning ($\Delta l = 0$ and $\Delta l = 5$). It should be noted that these dependencies result from numerical simulations that give a well developed non-degenerate oscillation, whose dynamics have reached their established regime. Thus, they represent the non-linear regime of oscillation [7] rather than the threshold of oscillation, which is usually considered within the linear stability analysis [6].

It is clear from the data of Fig. 9 that in the case of an imperfect phase matching the threshold of bifurcation becomes considerably smaller than that for $\Delta l = 0$. The other consequence of Fig. 9 is that the bifurcation in the oscillation spectrum occurs more easily in a cavity with relatively high losses ($R \rightarrow 0$) than in a cavity with a highly reflecting end mirror ($R \rightarrow 1$).

Thus the simulations show that the phase mismatch of the recorded gratings introduced by a slight angular deviation of the pump beams from collinearity results in a lower value of the threshold coupling strength for non-degenerate as well as for degenerate oscillation. The dynamics of the system, in particular the beat frequency, depends on the value of the mismatch.

4   Comparison with experimental results

We performed experiments with the semilinear oscillator in order to study the dependence of the beat frequency on the misalignment of the pump waves. The experimental set-up is the same as that described in [12]. The photorefractive crystal is a cobalt-doped barium titanate; the interaction length l of the two counterpropagating waves is close to 5 mm.

The evaluation of the coupling strength of our crystal has been conducted with a classical two beam coupling experiment with a reflection configuration for which the orientation and the grating spacing are the same as those in the semilinear oscillator. A value of $\gamma l = 3.9$ was measured, which is obviously underestimated because of a non-negligible depletion of the pump wave due to the strong light-induced scattering. To get a more realistic estimate of the coupling strength the linear polarization of the pump wave was rotated to 45° to decrease the coupling strength two times ($\cos^2 45°$ times). With the coupling strength which is reduced two times the light induced scattering is strongly inhibited and the pump depletion becomes much less important as well. By this manner a value of $\gamma l/2 \simeq 2.5$ is obtained, i.e., $\gamma l \approx 5$. Thus, the coupling strength of our sample is in a range where a non-degenerate oscillation may occur according to the simulations (Figs. 5–7) and where it should be impossible for $\Delta l = 0$ [6].

The experimental adjustment of the small misalignment angle and the calibration of the angular misalignment present practical difficulties. The precision of the pump beam alignment is limited by several factors. First, the two pump waves are loosely focused in the sample with converging lenses of focal distance $F = 1$ m. Second, the illumination of the sample with focused beams results in a non-uniform local heating [13] and therefore in the appearance of a converging thermal lens. This lens may be the reason for a further misalignment of the pump waves, especially if they are laterally shifted with respect to the other. The divergence of the pump wave transmitted through the sample, which is affected by both these factors is about 1.4 mrad. Therefore, it is reasonable to expect that the precision of the pump waves alignment is not better than 0.7 mrad, and that the oscillator should be insensitive to an angular mismatch much smaller than the pump divergence. In fact the oscillation dynamics show considerable changes with the misalignment angle even when it is one order of magnitude smaller than the pump beam divergence. Thus a high angular divergence does not exclude the possibility to measure the dependencies of the oscillation intensity and of the beat frequency on the misalignment angle, but with an uncertain knowledge of the zero position (i.e., a precise adjustment position).

Figure 10 shows the measured pump ratio dependence of the oscillation spectrum that agrees well with those reported previously in [8, 9, 12]. The pump waves are adjusted in this experiment to be nearly counterpropagating. It is obvious that the experimentally measured dependence is qualitatively very close to the result of the simulation presented in Fig. 8.

In a second set of experiments the dependencies of the beat frequency and the oscillation intensity on the misalignment angle have been investigated, the results are shown in Fig. 11. As one can see a deliberate misalignment as small as 0.01 mrad induces a remarkable change of the oscillation dy-
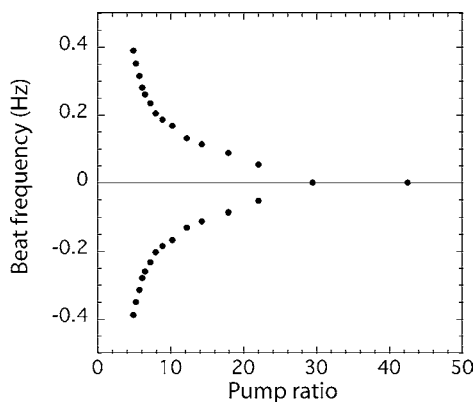

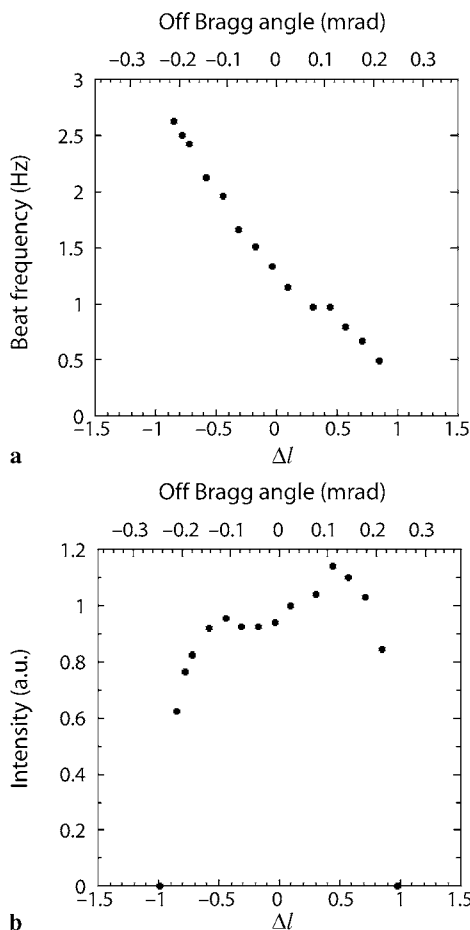**FIGURE 10** Experimentally measured dependencies of the oscillation spectrum on the pump ratio

FIGURE 11 Experimental dependencies of (**a**) beat frequency and (**b**) oscillation intensity on Δl. The upper axis gives the deviation angle from collinearity

namics. Such a sensitivity has already been mentioned in our recent publication on the oscillator with a frequency shifted feedback [14] and is the reason that led us to include the off-Bragg parameter in the model.

The oscillation intensity at first increases with the misalignment, it reaches a maximum and then drops down to zero quite abruptly (Fig. 11b). This is in qualitative agreement with the results of simulations for all the parameters that were tested (Figs. 5b, 6b, and 7b). The similarity of the cal-

culated and measured misalignment dependencies of the beat frequency is less evident. The variation of the beat frequency is nearly linear in Δl. There is however a shoulder and even a shallow minimum not far from the zero misalignment, which allows to claim that the beat frequency increases with the misalignment regardless of the sign of misalignment. The shape of the curves in Fig. 11a (its shoulder) and in Fig. 11b are experimentally reproducible. The reasons for this incomplete correspondence of the measured and calculated data can be due to the complex spatial structure of the oscillation waves (deviation from the plane wave approximation of the theory), and also the possibility for the system to choose other approximate phase matching conditions that are different from that shown in Fig. 3.

Due to the difficulty of obtaining a precise adjustment of the zero detuning as discussed above, the values in the abscissa are given with an additive uncertainty factor which in no way can exceed one half of the pump beam divergence, $|\Delta l| \leq 4$. With such a factor taken into account it is also not excluded that $\Delta l = 0$ is located beyond the area of oscillation existence so that the dependencies presented in Fig. 11a, b could correspond to one of the two lobes that are symmetric with respect a zero detuning (as shown in the simulations in Figs. 5 and 6). No clear arguments can be given however for the suppression of the oscillation in the symmetric lobe with an opposite Δl.

5   Conclusion

In conclusion, we emphasized the influence of the phase mismatch on the dynamics of the coherent semilinear oscillator. A relatively small misalignment of the two counter-propagating pump waves (on the order of a fraction of milliradian) affects considerably the threshold, the output and the temporal dynamics of the semilinear photorefractive coherent oscillator. For small misalignment the threshold of non-degenerate oscillation in coupling strength decreases with the increase of Δl, which may be expected qualitatively because the phase conjugate reflectivity becomes larger out of exact phase matching [5]. The decrease of the threshold results in the increase of the output oscillation intensity.

The most striking discovered effect consists in a very strong sensitivity of the oscillation dynamics on the pump beam misalignement. It is shown, both by simulation and experimentally, that the misalignment allows a non-degenerate oscillation for moderate values of the coupling strength ($\gamma l \leq 2\pi$) where a degenerate oscillation should occur with a perfect alignment [6].

An important issue of the presented simulation consists of possible different interpretations of the mismatch $\boldsymbol{\Delta}$ introduced in the set of equations of (22)–(26). We considered the pump misalignment as a source of such a mismatch and imposed the condition that the oscillation waves also become misaligned in a way to minimize the overall mismatch. In fact, the orientation of the oscillation waves is not predetermined by any condition apart from the boundary condition (reflection from the conventional mirror of the cavity) and it might happen that the oscillation waves will self-develop with an overall mismatch $\boldsymbol{\Delta}$ different from that considered in this paper. It is also not excluded that the oscillation waves 3 and 4 will self-bend to create a certain mismatch even in the case of perfectly aligned pump waves. Further studies are necessary to elucidate this last point.

The described high sensitivity of the oscillation to the angular mismatch may serve as a basis for the development of a sensor to detect small variations in the propagation direction of the laser beam. Such a sensor would require however pump beams with much smaller divergence as compared to those used in the present experiment.

REFERENCES

1 B. Fischer, S. Sternklar, S. Weiss, IEEE J. Quantum Electron. **QE-25**, 550 (1989)
2 M. Cronin-Golomb, B. Fischer, J.O. White, A. Yariv, IEEE J. Quantum Electron. **QE-20**, 12 (1984)
3 L. Solymar, D.J. Webb, A. Grunnet-Jepsen, *The Physics and Applications of Photorefractive Materials* (Clarendon Press, Oxford, 1996)
4 N.V. Kukhtarev, T.I. Semenets, K.H. Ringhofer, G. Tomberger, Appl. Phys. B **41**, 259 (1986)
5 C. Denz, J. Goltz, T. Tschudi, Opt. Commun. **72**, 129 (1989)
6 P. Mathey, M. Grapinet, H.R. Jauslin, B. Sturman, D. Rytz, S. Odoulov, Eur. Phys. J. D **39**, 445 (2006)
7 M. Grapinet, P. Mathey, H.R. Jauslin, B. Sturman, D. Rytz, S. Odoulov, Eur. Phys. J. D **41**, 363 (2007)
8 P. Mathey, S. Odoulov, D. Rytz, J. Opt. Soc. Am. B **19**, 2967 (2002)
9 P. Mathey, S. Odoulov, D. Rytz, Phys. Rev. Lett. **89**, 053 901 (2002)
10 J. Goltz, F. Laeri, T. Tschudi, Opt. Commun. **64**, 63 (1987)
11 P. Mathey, M. Grapinet, H.R. Jauslin, J. Opt. Soc. Am. B **24**, 860 (2007)
12 M. Grapinet, P. Mathey, S. Odoulov, D. Rytz, Appl. Phys. B **77**, 551 (2003)
13 P. Mathey, S. Latour, P. Lompré, P. Jullien, D. Rytz, B. Salce, Appl. Phys. B **71**, 523 (2000)
14 R. Rebhi, P. Mathey, H.R. Jauslin, S. Odoulov, Opt. Express **15**, 17 136 (2007)